Check for updates

MXene-based aptasensors: a perspective on recent advances

Navid Rabiee [ID] *[a] and Mohammad Rabiee [ID] *[b]

Recent advancements in science and technology have significantly enhanced public health by integrating novel materials and early diagnostic methods. A key focus is on MXenes, a class of materials known for their distinctive morphology and exceptional stability in diverse environments. MXenes possess notable structural engineering capabilities, enabling their design and synthesis into various forms tailored for specific applications. Their surface can be functionalized with different groups to enable chemical binding and physical attachment to various molecules, while variations in layer thickness and elemental composition influence their electrical conductivity and stability. This perspective article examines recent structural innovations in MXenes, particularly their application in biosensors. We highlight the role of aptamer surface decorations, which offer specific and selective binding for detecting a broad spectrum of analytes, thus underscoring MXenes' potential in advancing diagnostic technologies and improving public health.

1. Introduction

The progress of science and technology in the field of the emergence of new materials as well as its combination with new early diagnostic methods can greatly help public health and raise the level of health of human societies.[1,2] Meanwhile, the use of materials that have the ability to engineer physical and chemical properties is very important. MXenes are of interest due to their unique morphology, as well as their remarkable stability in different environments. This class of materials has structural engineering capabilities, they can be designed and synthesized in different forms for different applications.[3,4] MXene can be synthesized with different functional groups on the surface that provide the ability to chemically bind and physically attach to the surface with different molecules. Also, MXene can be synthesized in different layer thicknesses with different elements, which leads to different electrical conductivity as well as specific chemical and physical stability.[5–7] As healthcare challenges become increasingly complex, the demand for advanced materials that can address these issues has never been greater. Among these, the engineering of materials with tailored physical and chemical properties is particularly crucial. MXenes, a class of two-dimensional transition metal carbides and nitrides, have garnered considerable attention due to their unique morphology and remarkable stability in various environments. These materials possess exceptional structural engineering capabilities, allowing them to be designed and synthesized in diverse forms for a range of applications. Importantly, MXenes can be functionalized with various surface groups, which enhances their ability to chemically bond and physically interact with different molecules, facilitating their use in numerous fields, including biomedicine and environmental sensing.[8–10] In this perspective, we will focus on recent structural advancements in the MXene field, with the specific application in the biosensors. In this regard, aptamer surface decorations have been selected as the specific and selective binding molecules to detect a wide range of analytes.

2. Aptamer science and technology

Nucleic acids, commonly recognized for their role as carriers of genetic information essential for growth, development, and replication, possess remarkable versatility beyond just encoding life.[11] These molecules, particularly RNA, have the ability to fold into intricate 3D structures, known as ribozymes, which are capable of catalyzing biochemical reactions, regulating gene activity, mediating cellular responses, and facilitating protein synthesis.[12] Although the biological relevance of these folded RNA structures has been understood for some time, it wasn't until advancements in laboratory techniques—such as the ability to create vast libraries of random nucleic acid sequences and amplify them through polymerase chain reaction (PCR)—that scientists were able to evolve nucleic acids for tasks beyond their natural roles.[13] This breakthrough led to the creation of functional nucleic acid molecules designed to

[a]Department of Biomaterials, Saveetha Dental College and Hospitals, SIMATS, Saveetha University, Chennai 600077, India. E-mail: nrabiee94@gmail.com
[b]Biomaterial Group, Department of Biomedical Engineering, Amirkabir University of Technology, Tehran, Iran. E-mail: mrabiee@aut.ac.ir

bind specific targets or catalyze chemical reactions. These engineered nucleic acids, termed aptamers (derived from the Latin word for "fit"), can be tailored to interact with a diverse range of targets, from small molecules to entire cells.[14]

The technique used to isolate aptamers is known as SELEX (Systematic Evolution of Ligands by Exponential Enrichment),[15] an iterative process of selection and amplification that mimics natural evolution. SELEX begins with large pools of random nucleic acid sequences, often containing over a trillion distinct molecules, which are tested for their ability to bind to a specific target under controlled conditions (Fig. 1). Sequences that successfully bind are separated from those that don't, and the selected molecules are amplified to create a new, more enriched pool of functional sequences.

Nucleic acids are ideal candidates for this process because their sequences can be copied and passed on, allowing for the continuous refinement of their functional characteristics. This ability to replicate and improve selected molecules through directed evolution is a unique advantage of nucleic acids, as most other organic molecules lack a similar genotype-phenotype relationship.[16,17] Aptamers bind selectively to specific targets through their unique three-dimensional structures. This specificity arises from various non-covalent interactions, including hydrogen bonding, van der Waals forces, electrostatic interactions, and hydrophobic effects. As aptamers fold, they adopt structural motifs—such as loops, bulges, and helices—that complement the physical and chemical features of the target molecule's surface. This precise fit enable
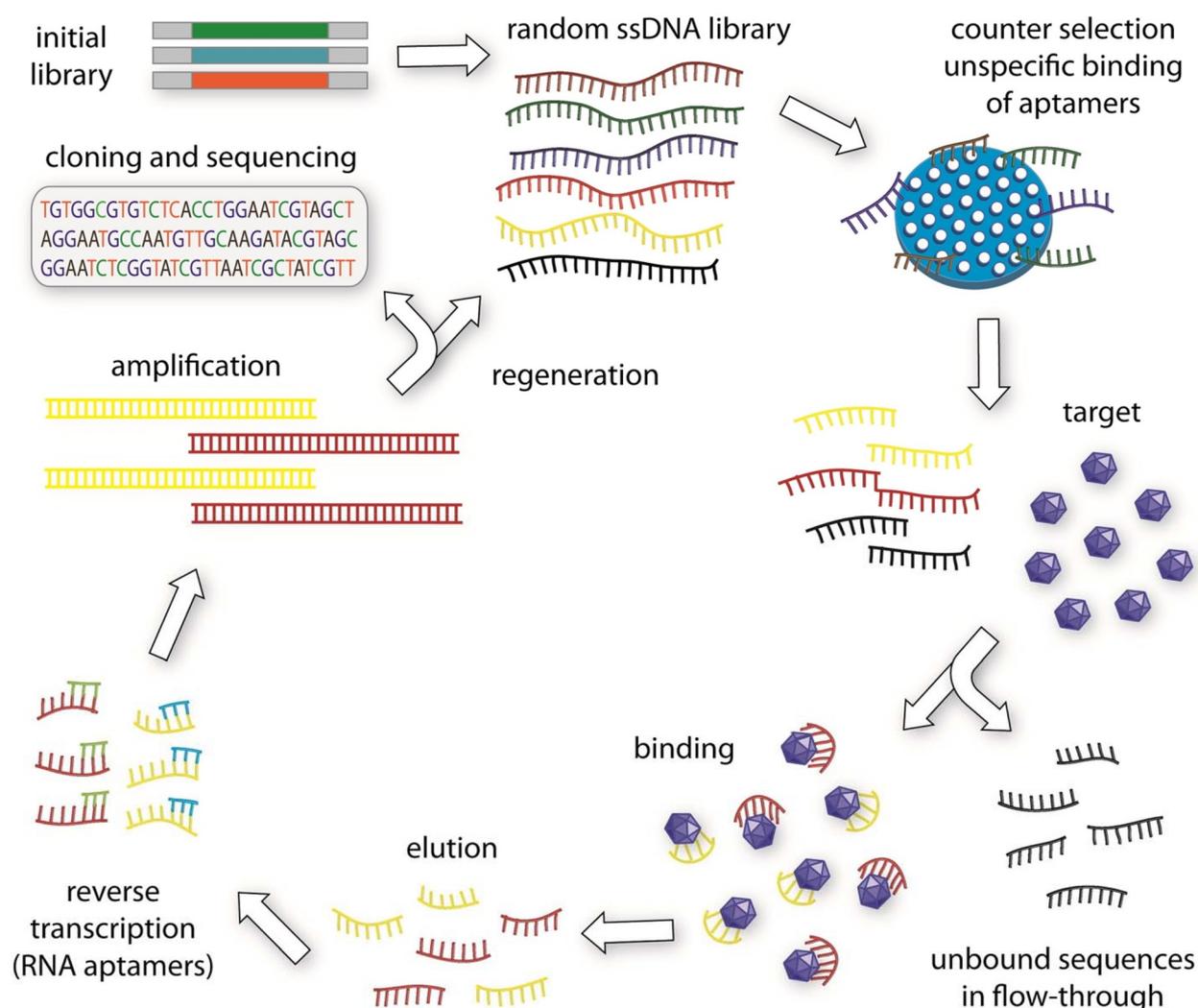

Fig. 1 The conventional SELEX process for generating aptamers begins with the creation of an initial oligonucleotide library. This library is then subjected to a selection process. Typically, the first step in conventional SELEX protocols involves a counter-selection against the matrix where the target molecule is immobilized, ensuring that any non-specifically bound aptamers are removed. The remaining pool of oligonucleotides is then incubated with the target molecule. Sequences that do not bind are discarded, while those that bind to the target are retained. For RNA aptamers, these bound oligonucleotides are reverse transcribed into DNA, followed by amplification through PCR. After several rounds of this selection and amplification process, the sequences are cloned and sequenced. The enriched aptamers are then evaluated for their binding affinity to the target molecule. Reprinted (reproduced) with permission from ref. 16, Copyright 2015, Elsevier.

aptamer to recognize and bind tightly to specific sites on the target, much like antibodies, but with the advantage of forming highly customizable and flexible structures. This adaptability allows aptamers to distinguish between closely related molecules, achieving high levels of selectivity even for subtle structural differences. Through these interactions, aptamers achieve robust binding, making them invaluable tools in biosensing and targeted therapeutic applications.

Aptamers are frequently compared to antibodies, as both serve as tools for binding and detecting specific targets. However, aptamers offer several advantages over traditional antibodies and other protein-based affinity reagents. Aptamers can be synthesized in large quantities using chemical processes, bypassing the biological production methods that sometimes lead to issues with contamination or variability seen in antibody manufacturing. Moreover, aptamers tend to provoke less of an immune response compared to protein-based therapeutics, and their small size allows them to reach areas of the body that are inaccessible to larger antibodies. Another key advantage is that aptamers can be chemically modified to fine-tune their clearance from the body and control their half-life, providing flexibility in their therapeutic applications. Aptamers can also be swiftly deactivated using antisense oligonucleotides, which are designed to bind and neutralize the aptamer's functional domain—a feature that offers precise control over their activity. Furthermore, unlike antibodies, aptamers do not require cold storage in a few cases. They can be refolded into their functional form after being stored at room temperature, reducing shipping and handling costs associated with cold-chain logistics.[18–20] The ability to engineer aptamers into molecular devices that respond only in the presence of specific targets has sparked significant interest in their use for diagnostic applications. Their compatibility with other nucleic acid technologies, such as DNA amplification, nanotechnology, and computing, has further expanded their utility in a range of scientific fields. This adaptability, combined with their ease of production and modification, positions aptamers as powerful tools with immense potential for therapeutic and diagnostic applications.[21]

Aptamers, akin to antibodies, hold substantial promise for therapeutic and diagnostic applications. These nucleic acid molecules, once bound to their specific targets, can act as either stimulators or inhibitors, depending on their inherent properties. Aptamers offer distinct advantages over antibodies in drug development. They generally exhibit lower immunogenicity, longer shelf life, easier quality control, and the ability to undergo reversible pharmacological changes through complementary oligonucleotides.[22] To qualify as effective clinical drugs, aptamers must not only demonstrate robust targeting and specificity—achieved through the SELEX process—but also meet additional criteria such as cost-effectiveness, enhanced serum stability, and sufficient bioavailability.[23] A significant challenge in using aptamers for *in vivo* applications is their stability in serum. While chemical modifications or non-natural nucleotide analogues can be introduced to improve the stability of aptamer libraries during SELEX, these

modifications can also be applied to already selected aptamers.[24] However, predicting how these modifications will impact the aptamer's three-dimensional structure remains complex due to current limitations in structural prediction technologies. As a result, modifications are often introduced incrementally, with each change being experimentally tested for its effects.[25,26] Surprisingly, certain chemical modifications, not only enhance the aptamers' resistance to nucleases but can also improve their binding affinity. This increased affinity is believed to stem from greater thermal stability of the aptamer's tertiary structure.[27,28] Unlike antibodies, which maintain structural stability across various conditions, aptamers can have their binding affinity significantly affected by environmental factors such as temperature, pH, and ion concentration. For instance, the thrombin-binding aptamer (TBA15) only adopts its functional conformation in the presence of potassium ions, illustrating how environmental conditions can influence aptamer function.[29,30]

Recent advancements have shown that systematic efforts to enhance the thermal stability of aptamers could greatly benefit their application in various fields. Techniques like error-prone PCR, aptamer affinity maturation, and site-directed mutagenesis have been employed to improve aptamer binding properties.[31–33] For example, researchers have successfully developed mutant versions of a VEGF-binding aptamer with up to 16 times greater affinity than the original.[34] Similarly, constructing bivalent or multivalent aptamers, which involve linking multiple aptamers or combining different ones, can improve binding sensitivity and biological function.[35] However, the effectiveness of multivalent aptamers does not always scale linearly with the number of subunits, requiring careful experimental optimization. Additionally, the small size of typical aptamers, which ranges from 25 to 40 nucleotides and weighs between 8250 and 13 200 Da, results in rapid renal clearance after systemic administration.[36] To counteract this, strategies such as increasing the aptamer's molecular size through polyethylene glycol (PEG) attachment or incorporating it onto nanoparticles have been employed to reduce renal clearance and extend circulation time. For instance, the FDA-approved aptamer drug Macugen, which uses a 40 kDa PEG, has shown a plasma half-life of 9.3 hours, making it suitable for clinical use. Integrating techniques like PEGylation and constructing polyvalent aptamers can enhance the drug-like properties of aptamers, including their binding affinity and bioavailability. Although post-SELEX modifications remain challenging due to the complexity of predicting their effects on aptamer structures, they offer valuable opportunities for developing aptamer-based therapeutics.[37–40]

3. MXene structures and advancements

Since the discovery of Ti_3C_2 in 2011,[41] there has been remarkable progress in the study of the synthesis, characterization, and potential applications of two-dimensional (2D) carbides

and nitrides, commonly referred to as MXenes. An influential 2012 publication in ACS Nano highlighted the synthesis of M_2X, M_3X_2, and M_4X_3, marking the emergence of an extensive new category of 2D materials.[42] The structural variety within this class expanded further with the introduction of M_5C_4,

detailed in a 2020 ACS Nano article. MXenes generally follow the formula $M_{n+1}X_nT_x$, where M is a transition metal, X denotes carbon or nitrogen, n ranges from 1 to 4, and T_x represents surface terminations on the outermost transition metal layers (Fig. 2). The potential for ordering metal atoms
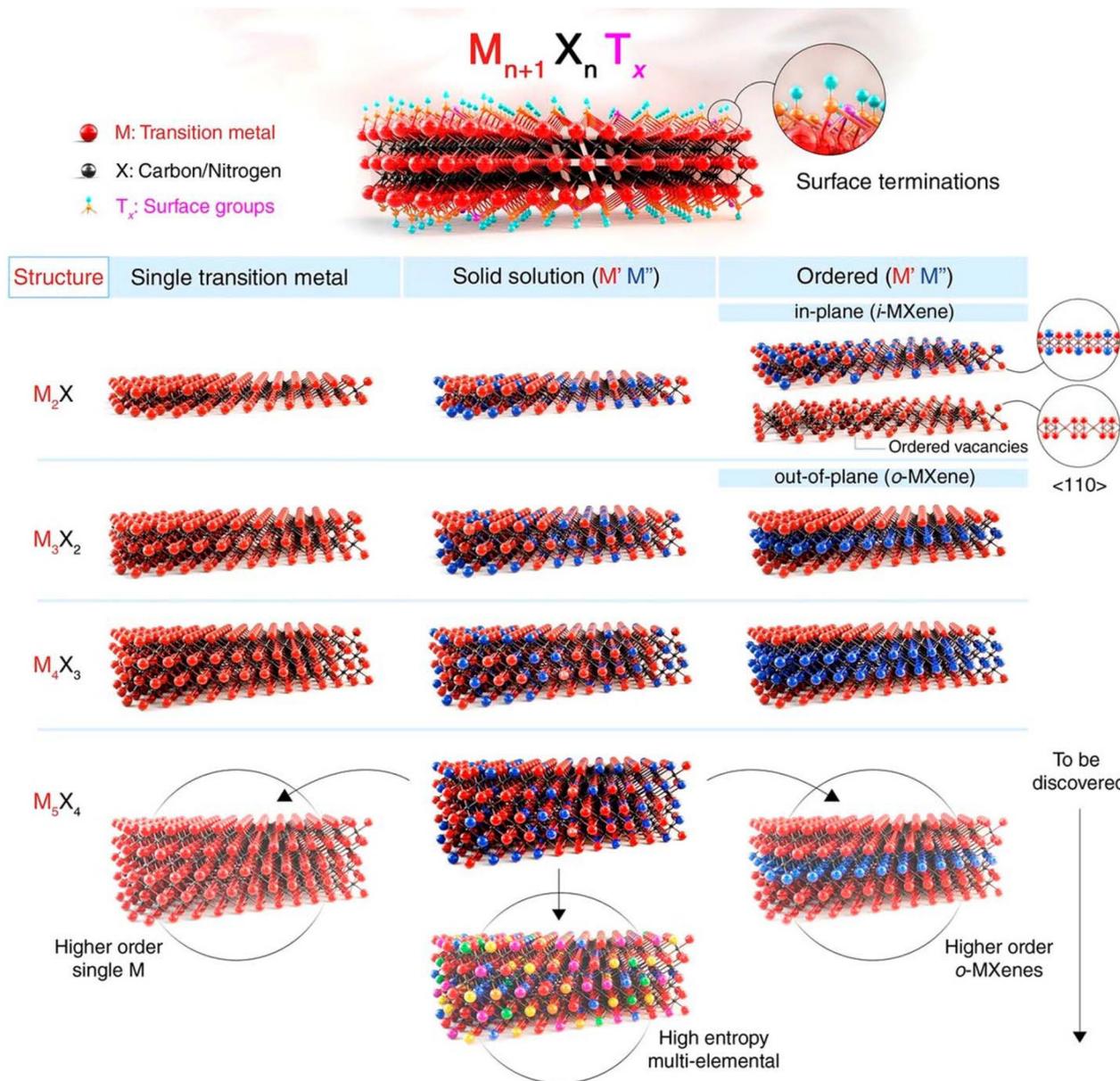

Fig. 2 The diagram illustrates the structural configurations observed in MXenes, which are defined by the formula $M_{n+1}X_nT_x$. In this notation, M denotes a transition metal, X represents nitrogen and/or carbon, and Tx refers to surface terminations on the metal layers. The number of metal and nitrogen/carbon layers in a MXene's structure is indicated by the value of n, which ranges from 1 to 4. Examples of MXenes include Ti_2CT_x ($n = 1$), $Ti_3C_2T_x$ ($n = 2$), $Nb_4C_3T_x$ ($n = 3$), and $(Mo,V)_5C_4T_x$ ($n = 4$). Recent discoveries have identified $Mo_4VC_4T_x$, a unique solid solution MXene with five metal layers and twinning within these layers, which deviates from previously known MXene forms. Solid solutions or ordered structures can emerge when multiple transition metals occupy the M sites in MXenes. These configurations include in-plane ordered structures (i-MXenes) like $(Mo_{2/3}Y_{1/3})_2CT_x$, in-plane vacancy structures like $W_{2/3}CT_x$, and out-of-plane ordered varieties, known as o-MXenes. In o-MXenes, two key configurations exist: one with a single M″ transition metal layer sandwiched between two M′ layers, such as $Mo_2TiC_2T_x$, and another with two M″ layers between two M′ layers, as in $Mo_2Ti_2C_3T_x$. Further possibilities, such as structures with one or three M″ layers within the M_5X_4 configuration, are still under investigation. The diagram also highlights unconfirmed potential structures, including high-entropy MXenes and higher-order single M or o-MXenes. Reproduced with permission from ref. 45. Copyright 2021 Science.

both in-plane and out-of-plane results in over 100 possible structures. This number is greatly expanded by the presence of surface terminations and the ability to form solid solutions on both the M and X sites, along with mixed terminations, paving the way for a nearly limitless array of 2D materials with unique properties.[43,44]

The discovery of remarkable properties in single-layer and few-layer graphene sparked widespread interest in various other 2D materials.[46,47] Initial research primarily focused on exfoliating van der Waals-bonded solids like BN and transition metal dichalcogenides. However, 2D structures of silicon and germanium, which do not have van der Waals-bonded layered precursors, were later demonstrated. In 2011, the development of MXenes—2D carbides and nitrides of transition metals—emerged through the selective etching of strongly bonded layered solids such as MAX phases. MXenes distinguish themselves from the numerous existing 2D materials by providing metallic electrical conductivity, a trait largely absent from most other 2D materials, which tend to be semiconductors, semimetals, or dielectrics. MXenes exhibit conductivity values as high as $20\,000$ S cm^{-1}, along with superior strength and stiffness when compared to other solution-processed 2D materials. They can be produced on a large scale, with batch sizes reaching kilograms, and offer sufficient environmental stability to support a wide range of applications. Additionally, MXenes are biocompatible and can be processed in aqueous solutions without the need for surfactants. These materials behave like hydrophilic, water-dispersible 2D metals or electrically conductive clays, as their rheological properties are similar to clay. With dozens of MXenes already available and an infinite number of potential compositions, their properties can be further fine-tuned through reversible chemical or electrochemical intercalation, applied potential, or illumination. While MXenes display metallic conductivity, their Fermi levels can be adjusted by external factors, mimicking behavior typically seen in semiconductors. The unique combination of MXenes' properties makes them suitable for a diverse array of applications. Their conductive and redox capabilities make them ideal for energy storage, while their conductivity and catalytic abilities support electrocatalysis. The pairing of conductivity with transparency is essential for transparent conductors and heaters, while conductivity combined with color enables use in photonic and optoelectronic devices. Additionally, tunable plasmon resonance allows for applications in photothermal therapy, photocatalysis, and surface-enhanced Raman spectroscopy.[48–52]

The creation of i-MXenes, which include structured vacancies such as Ti_4C_3, Ti_5C_4, and $Mo_4VC_4T_x$, has been successfully achieved. In addition, nanometer-thin Mo_2C films have been grown through chemical vapor deposition (CVD). Multiple solid solution MXenes have also been synthesized, and carbide MXenes have been successfully converted into nitrides via high-temperature ammonia treatment. Similarly, transition metal dichalcogenides (TMDs) have been topochemically transformed into 2D nitrides like Mo_5N_6 and W_5N_6, suggesting a promising route for the synthesis of additional 2D carbides and nitrides. These advancements could greatly benefit from high-throughput simulations and machine learning to accelerate the discovery of new materials.[53–55]

Research and predictions have also expanded beyond MXenes, encompassing a variety of new 2D materials with unique chemical compositions. This includes 2D MC_2 carbides, such as TiC_2 (pending experimental verification), ultrathin MAX phases (also known as MAXenes), vapor-grown 2D $MoSi_2N_4$, and a newly introduced class of 2D borides called MBenes, where boron replaces the X element in the MXene formula. Some of these predictions have been partially confirmed, leading to the exfoliation of particles or the growth of ultrathin crystals. Electrically conductive materials, like carbide and nitride electrides (e.g., Ca_2N), are also gaining attention for their notable physical properties, despite challenges with environmental stability. For example, 2D $MoSi_2N_4$ grown in gas exhibits an impressive Young's modulus of approximately 0.5 TPa and a breaking strength of 66 GPa.[56–59]

Density functional theory (DFT) calculations have provided insights into a wide range of semiconducting 2D structures with the general formula MA_2Z_4. In these structures, M represents a transition metal, A can be Ge or Si, and Z varies between elements like N, P, or As. Computational studies have also highlighted the potential of 2D MC_2 carbides, such as NbC_2, TaC_2, and MoC_2, across numerous applications, including biomedical sciences and catalysis, particularly in oxygen evolution reactions (OER) and hydrogen evolution reactions (HER). In the realm of electrocatalysis, partially etched borides have shown promise for HER applications. Like MAX phases, the bonds between M and A elements in MAB phases are weaker compared to M–B bonds, which suggests the possibility of selective etching of A-elements. However, previous efforts have resulted in multilayer MBenes with stacking faults caused by partial removal of aluminum layers, hindering further exfoliation. As a result, continued research is needed to identify suitable precursors and achieve complete exfoliation of MAB phases into MBenes.[60–66]

4. Aptamer decorated MXene biosensors: cutting-edge studies

The yellow fever virus (YFV) is an acute infectious virus that poses significant risks of high morbidity and mortality, particularly during its toxic phase. Given the absence of precise treatment for YFV, early detection and intervention are critical. To address this need, a miniaturized and highly sensitive electrochemical biosensor was developed, specifically designed to detect YFV.[67] This biosensor incorporates a heterolayer composed of a truncated DNA aptamer and MXene, which significantly enhances its performance. The YFV NS1 aptamer was synthesized using the SELEX (Systematic Evolution of Ligands by Exponential Enrichment) technique, allowing it to specifically target and bind to the YFV NS1 protein. The integration of MXenes into the biosensor design improves its electrical sensitivity while expanding the surface area for aptamer attach-

ment, thereby boosting detection capabilities. Additionally, the truncation of the aptamer reduces production costs, making the biosensor more practical for widespread use. The biosensor's performance was rigorously tested using electrochemical methods, including cyclic voltammetry (CV) and electrochemical impedance spectroscopy (EIS). Its limit of detection (LOD) was determined to be 2.757 pM in phosphate-buffered saline (PBS) and 2.366 pM in 10% human serum, demonstrating its high sensitivity and specificity in binding to the YFV NS1 protein over other proteins. Further analysis of the biosensor's surface characteristics was conducted using atomic force microscopy (AFM) and EIS. These studies confirmed the effective immobilization of each material within the biosensor and highlighted its enhanced detection performance. The miniaturized design and superior sensitivity make this biosensor a promising tool for the early diagnosis of YFV, providing timely intervention opportunities and aiding in the control and prevention of yellow fever outbreaks. Its high specificity and potential for rapid, efficient detection position it as a valuable asset in both clinical and field settings.

Electrochemical aptamer-based (E-AB) sensors are emerging as promising tools for real-time biomarker monitoring due to their exceptional selectivity and versatility in detecting various proteins and small molecules. Despite their potential, most E-AB sensors currently rely on planar gold structures, which limit both their sensitivity and operational stability, particularly in continuous monitoring applications. While the use of gold nanostructures has improved sensor performance, there has been little exploration into combining gold nanostructures with other nanomaterials for enhanced continuous molecular detection. To address this limitation, a novel E-AB sensor was developed using a nanocomposite of gold nanoparticles and MXene Ti$_3$C$_2$ (AuNPs@MXene), targeting vascular endothelial growth factor (VEGF), an essential signaling protein in humans.[68] The introduction of this nanocomposite resulted in significant improvements in sensor performance, with over thirty-fold and half-fold increases in active surface area compared to bare and gold nanoparticle-modified electrodes, respectively. These enhancements translated into heightened analytical capabilities for continuous biomarker monitoring. Through systematic optimization and characterization, the newly designed E-AB sensor demonstrated remarkable improvements in both stability and sensitivity, thanks to the incorporation of the AuNPs@MXene nanocomposite. This approach also facilitated more robust signal integrity and reduced noise during high-frequency, continuous monitoring, regardless of the buffer conditions or reporter types used.

Organic electrochemical transistors (OECTs) with signal amplification and enhanced stability are anticipated to play a vital role in detecting environmental pollutants. However, traditional designs can expose sensitive biomolecules to the gate's bias voltage, potentially affecting their activity. To overcome this limitation, a novel organic photoelectrochemical transistor (OPECT) aptamer biosensor was developed for detecting di(2-ethylhexyl) phthalate (DEHP).[69] This innovative sensor integrates photoelectrochemical analysis with organic electrochemical transistor technology. The sensor design incorporates MXene/Bi$_2$S$_3$/CdIn$_2$S$_4$ as the photoactive material, which drives the photoelectrochemical processes (Fig. 3). Signal amplification is achieved through a target-dependent DNA hybridization chain reaction, while Ru(NH$_3$)$_6$$^{3+}$ is used as a signal enhancement molecule. The OPECT biosensor, which utilizes poly(3,4-ethylenedioxythiophene) (styrenesulfonate) as its foundation, achieved an impressive current gain of nearly a thousand times at zero bias voltage, thanks to the modulation provided by the MXene/Bi$_2$S$_3$/CdIn$_2$S$_4$ photosensitive material. This "signal-on" OPECT sensing platform demonstrated highly sensitive and specific detection of DEHP, achieving a detection range of 1–200 pM and a minimum detection limit of 0.24 pM under optimized conditions. Its effectiveness was further validated by its successful application to real water samples, yielding satisfactory results.

In this study, a self-assembled sensing interface was successfully developed by functionalizing Ti$_3$C$_2$ MXene with an aptamer, effectively leveraging the excellent electrical properties of Ti$_3$C$_2$ MXene along with the aptamer's specific recognition capabilities.[70] The performance of this sensing interface was evaluated using two antibiotic residues, kanamycin, and tetracycline, as test cases. Under optimized conditions, the interface demonstrated a linear detection range from 100 fM to 1 μM and achieved an impressive detection limit of 1 fM. Additionally, the recovery rates for kanamycin ranged from 97.15% to 103.00%, while for tetracycline, they ranged from 99.559% to 106.36%. Moreover, the interface was able to detect changes in electrical signals resulting from the aptamer's specific recognition of the target molecules, indicating different sensing behaviors. This self-assembled sensing interface not only offers a new direction for the development of ultrasensitive detection technologies in food analysis but also provides valuable insights into the study of aptamer conformational changes.

A novel electrochemical aptamer-based sensing technique was developed using a PEI@Ti-MOF@Ti$_3$C$_2$T$_x$-MXene composite for the highly sensitive detection of ZEN in food samples. The titanium-based metal–organic framework (MOF), NH$_2$-MIL-125, was synthesized in situ using 2-aminoterephthalic acid as the organic ligand and tetrabutyl titanate as the metal center.[71] This synthesis was followed by the simultaneous integration of Ti$_3$C$_2$T$_x$-MXene to create the Ti-MOF@Ti$_3$C$_2$T$_x$-MXene composite. The resulting material was then functionalized with polyethyleneimine (PEI) and covalently attached to gold electrodes to form a sensing platform. By combining the MOF with MXene, the composite demonstrated superior electrochemical properties compared to the individual materials alone, while also reducing the stacking effect and increasing the availability of binding sites for the aptamer. The sensor achieved an impressive limit of detection (LOD) of 1.64 fg mL^{-1}. Additionally, the sensor successfully detected ZEN in cornmeal and beer samples, showcasing excellent stability, reproducibility, and selectivity. This innovative sensor highlights its potential for practical applications in quality control and food safety monitoring.
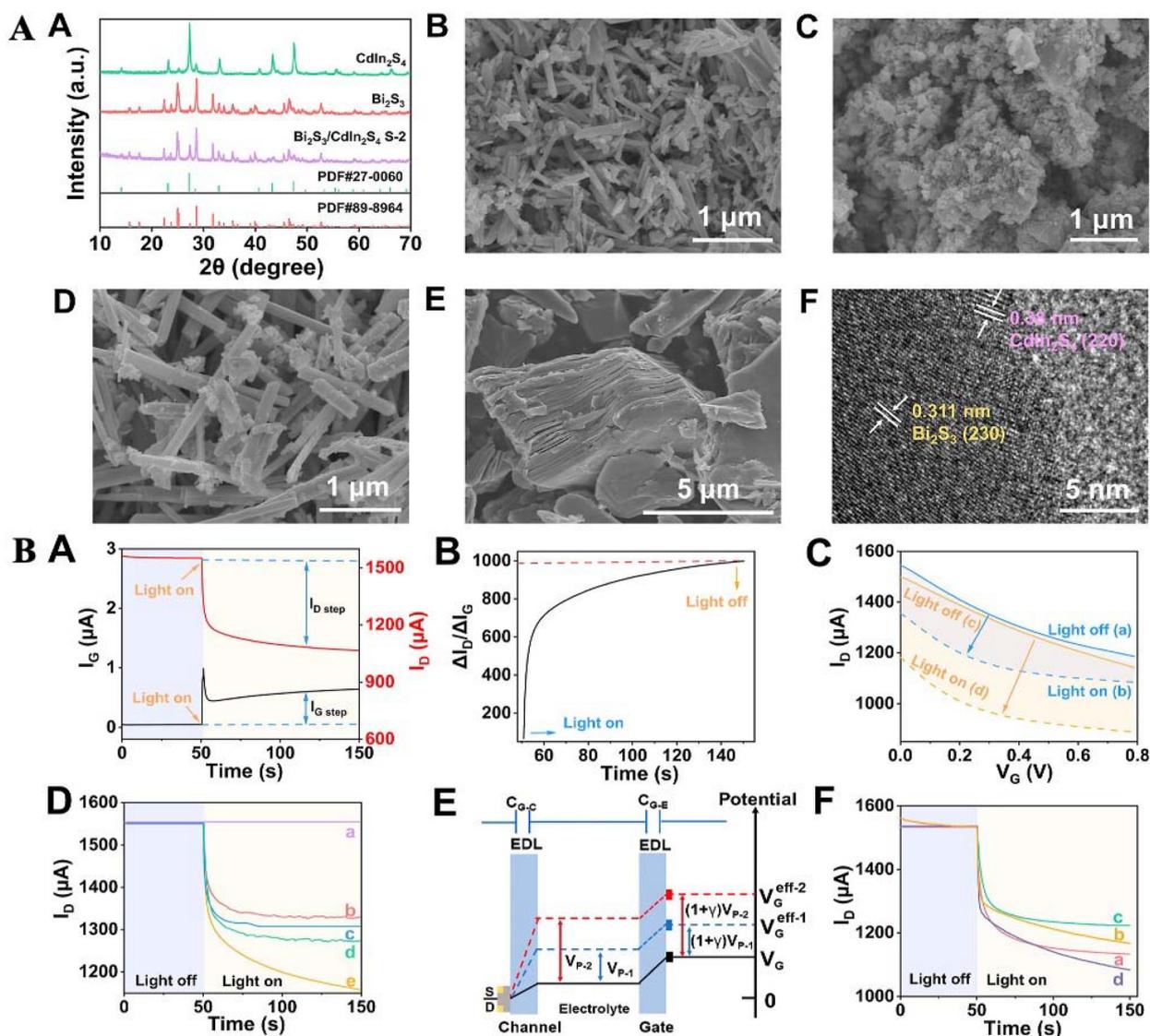
Fig. 3 (A) (A) X-ray diffraction (XRD) patterns were obtained for Bi_2S_3, $CdIn_2S_4$, and the $Bi_2S_3/CdIn_2S_4$ composite (labeled S-2). Scanning electron microscopy (SEM) images were captured for Bi_2S_3 (B), $CdIn_2S_4$ (C), the $Bi_2S_3/CdIn_2S_4$ composite (S-2) (D), and MXene (E). Additionally, a high-resolution transmission electron microscopy (HRTEM) image of the $Bi_2S_3/CdIn_2S_4$ composite (S-2) is shown (F). (B) (A) The time-dependent behavior of IG (black line) and ID (red line) was observed during light exposure. (B) The corresponding ratio of the ID step relative to the IG step was calculated. (C) Transfer curves for $Bi_2S_3/CdIn_2S_4$/ITO (blue lines) and MXene/$Bi_2S_3/CdIn_2S_4$/ITO (yellow lines) were recorded both with (dashed lines) and without (solid lines) light treatment in a 0.1 M Tris-HCl solution (VD = 0.1 V). (D) Time-dependent ID responses were measured for various materials, including (a) MXene/ITO, (b) $CdIn_2S_4$/ITO, (c) Bi_2S_3/ITO, (d) $Bi_2S_3/CdIn_2S_4$/ITO, and (e) MXene/$Bi_2S_3/CdIn_2S_4$/ITO. (E) A diagram illustrating the potential distribution and the working principle of the OPECT, starting with the initial $Bi_2S_3/CdIn_2S_4$/ITO configuration, then with and without light exposure, and finally after MXene treatment. (F) Stepwise ID responses were recorded for (a) MXene/$Bi_2S_3/CdIn_2S_4$/ITO, (b) TgRNA/MXene/$Bi_2S_3/CdIn_2S_4$/ITO, (c) H1−H2-TgRNA/MXene/$Bi_2S_3/CdIn_2S_4$/ITO, and (d) Ru/H1−H2-TgRNA/MXene/$Bi_2S_3/CdIn_2S_4$/ITO, all under zero gate bias. Reprinted (reproduced) with permission from ref. 69, Copyright 2024, American Chemical Society.

Rapid and efficient detection techniques for health-related biomarkers provide critical physicochemical insights necessary for disease diagnosis or general health assessment. Among these techniques, electrochemical detection of bio-macro-molecules, such as C-reactive protein (CRP), holds significant promise for diagnosing acute inflammation linked to infections, heart conditions, and more. In this work, a novel electrochemical aptamer biosensor was developed by combining

$Ti_3C_2T_x$ MXene with *in situ* reduced gold nanoparticles (AuNPs), enabling the immobilization of thiolated RNA aptamers for CRP detection.[72] Ferrocenecarboxylic acid (Fc (COOH)) was employed as a signal probe. The sensor's performance for CRP detection was optimized by adjusting various working conditions, such as incubation times and pH levels. The large surface area of $Ti_3C_2T_x$ MXene, combined with the excellent electrical conductivity of Au NPs, endowed

the sensor with high sensitivity across a broad linear detection range of 0.05–80.0 ng mL^{-1}, strong selectivity against interfering substances, and a low detection limit of 0.026 ng mL^{-1}. Furthermore, the sensor successfully detected CRP in serum samples using the spike and recovery method, achieving satisfactory recovery rates. These findings demonstrate the potential of this electrochemical aptamer biosensor for rapid and accurate CRP detection, highlighting its practical applicability in clinical and diagnostic settings.

Despite the availability of various methods for measuring digoxin, scientific advancements have allowed for the detection of even trace amounts of this drug. However, the high costs associated with previous methods have driven the development of more cost-effective techniques capable of measuring very low levels of digoxin. A new aptasensor was created by immobilizing a digoxin-specific aptamer onto a screen-printed carbon electrode (SPCE) modified with MXene and AuNPs using thioglycolic acid (TGA) as a linker (SPCE/MXene-AuNPs/TGA/Apt).[73] The physicochemical properties of the synthesized nanocomposite were analyzed using microscopic and voltammetry techniques. The combination of MXene, AuNPs, and TGA significantly increased the active surface area, promoting enhanced electron transfer, improving electrical conductivity, and boosting the stability and longevity of the aptasensor. This design allowed for a detection limit of 0.03 pM, calculated with a signal-to-noise ratio (S/N) of 3. Additionally, the biosensor demonstrated excellent stability, an extended shelf life, and a low per-sample detection cost of under 100 USD. Given these advantages, the authors suggest that the electrochemical biosensor, enhanced with MXene-AuNPs/TGA for improved signal amplification, represents a promising and cost-effective method for detecting digoxin in environmental samples.

Exosomes, small nanovesicles secreted by cells, are key players in various pathological processes and hold significant potential as tumor biomarkers due to their abundant release during tumor development. Developing a practical, efficient, and cost-effective method for simultaneously enriching and detecting exosomes is crucial for advancing both basic research and clinical applications. In this study, a magnetic Ti$_3$C$_2$-based composite material (Fe$_3$O$_4$@Ti$_3$C$_2$@PEI@DSP@aptamer@FAM-ssDNA) functionalized with aptamers was designed to achieve this dual purpose.[74] The composite utilizes CD63-specific aptamers to selectively capture and bind exosomes, which are then separated using magnetic techniques. The exosomes are released through the cleavage of disulfide bonds in DSP. Compared to traditional approaches, the Fe$_3$O$_4$@Ti$_3$C$_2$@PEI@DSP@aptamer@FAM-ssDNA composite demonstrated superior efficiency in enriching exosomes while maintaining their structural and functional integrity. Detection of the exosome concentration is achieved through fluorescence quenching by Ti$_3$C$_2$, coupled with competitive binding between the exosomes and a fluorescently labeled probe. This method demonstrated a detection limit of 4.21×10^4 particles per mL, comparable to the leading techniques in exosome detection. This study introduces a highly sensitive,

accurate, and cost-effective approach for the simultaneous enrichment and detection of exosomes, showing great promise for clinical research and diagnostic applications.

Personalized monitoring of female hormones, such as oestradiol, is crucial for fertility and women's health management. Traditional methods often involve invasive blood samples and bulky laboratory equipment, making them impractical for home use. This study introduces a wearable aptamer nanobiosensor designed for non-invasive, real-time monitoring of oestradiol through sweat analysis.[75] This sensor utilizes a target-induced strand displacement mechanism and incorporates a gold nanoparticle-MXene-based detection electrode for exceptional sensitivity. It achieves an ultra-low detection limit of 0.14 pM with a reagentless, amplification-free, and 'signal-on' approach. The fully integrated system autonomously induces sweat through iontophoresis, collects precise microfluidic sweat samples via capillary bursting valves, and performs real-time oestradiol analysis. It also calibrates results with additional data such as temperature, pH, and ionic strength, and communicates wirelessly with user interfaces like smartphones. Validation with human participants revealed cyclical fluctuations in sweat oestradiol levels during menstrual cycles and a strong correlation between sweat and blood oestradiol concentrations. Sensor performance was evaluated using square wave voltammetry (SWV) in artificial sweat containing physiologically relevant oestradiol concentrations (0.1–100 pM). The sensor demonstrated a log-linear response in peak current density with an ultra-low detection limit of 0.14 pM. It showed high selectivity for oestradiol over potential interferents at much higher concentrations. Accuracy was confirmed by comparing sensor results with enzyme-linked immunosorbent assay (ELISA) data from iontophoresis-induced sweat samples, yielding a high correlation coefficient of 0.921. To reduce incubation time, the study explored applying an external electric field (positive potential bias) to accelerate the competitive interaction and recapture processes. The application of a positive potential at the working electrode enhanced the transport of the redox probe, significantly reducing incubation time to 10 minutes. Electrochemical measurements indicated improved sensor performance with this bias, achieving a current flow of approximately 300 nA and maintaining low power dissipation. The sensor's signal primarily reflects the oestradiol-induced strand displacement reaction, with minimal contribution from electrostatic adsorption. The biosensor can be regenerated in deionized water or acidic conditions, showing only 6.2% signal drift after five cycles of repetitive measurements and regeneration. This innovative wearable sensor demonstrates significant potential for non-invasive, personalized hormone monitoring in practical applications.

The creation of an effective biosensor for diagnosing acute myocardial infarction (AMI) is critically important. However, detecting cardiac Troponin I (cTnI) poses significant challenges due to the complex nature and low concentration of cTnI in clinical samples. To address this, a novel aptamer-based biosensor utilizing MXene and multi-wall carbon nano-

tubes (MWCNTs) has been developed for the detection of cTnI.[76] This approach leverages the MXene/MWCNTs nanocomposite to achieve significant signal amplification, enabling the biosensor to cover a broad detection range from 10 to 10^6 pg mL^{-1}, with an exceptionally low detection limit of 6.21 pg mL^{-1}. The biosensor demonstrates excellent selectivity, reproducibility, and stability. It also exhibits a strong clinical correlation with a regression equation of $y = 1.202x + 0.0147$ and an R^2 value of 0.9797. A significant p-value difference is noted between AMI patients and healthy controls. The biosensor achieves an impressive area under the curve (AUC) of 0.981, with a sensitivity of 0.938 and a specificity of 0.923. These remarkable features and clinical performance make this aptamer-based biosensor an ideal tool for the practical monitoring of acute myocardial infarction.

A novel dual-modal electrochemical aptasensor, termed CoNi-MLDH@V$_2$CT$_x$, was developed for noninvasive point-of-care cortisol detection across various body fluids, including sweat, urine, and blood.[77] This design is based on the heterojunction between V$_2$CT$_x$ MXene nanosheets (NSs) and bimetallic CoNi-layered double hydroxide (CoNi-MLDH) (Fig. 4). The V$_2$CT$_x$ NSs served as scaffolds for the *in situ* growth of cobalt/nickel zeolitic imidazolate framework (CoNi-ZIF) polyhedrons, which were subsequently transformed into CoNi-MLDH NSs *via* an etching–coprecipitating process. The combination of V$_2$CT$_x$ NSs, known for their excellent electrochemical

activity, and CoNi-ZIF, with its large surface area, rich functionality, and strong bioaffinity toward aptamers, provided a powerful platform for constructing the aptasensor. This dual-modal system, which includes impedimetric sensing and a zinc-air battery-driven self-powered mode, exhibited an exceptional ability to detect cortisol across a broad concentration range from 10 fg mL^{-1} to 100 ng mL^{-1}, with ultra-low detection limits of 0.26 fg mL^{-1} and 0.17 fg mL^{-1}, respectively. The aptasensor demonstrated remarkable selectivity, stability, reproducibility, and regeneration capability, highlighting its potential for cortisol monitoring in diverse environmental conditions. This work presents a highly promising method for promoting mental health through sensitive and selective cortisol detection in human fluids.

An ultrasensitive ECL aptasensor was designed for the detection of the aminoglycoside antibiotic tobramycin (TOB) utilizing the chemiluminescence reaction between luminol and hydrogen peroxide (H$_2$O$_2$) in a basic solution.[78] The nanocomposite Ti$_3$C$_2$/Ni/Sm-LDH played a crucial role in catalyzing luminol oxidation and H$_2$O$_2$ decomposition, generating various reactive oxygen species (ROS) that significantly enhanced the ECL signal intensity, allowing for accurate TOB concentration measurement. To assess the aptasensor's performance and the efficacy of the synthesized nanocomposite, CV and EIS techniques were employed. The Ti$_3$C$_2$/Ni/Sm-LDH nanocomposite exhibited a large surface area, numerous active
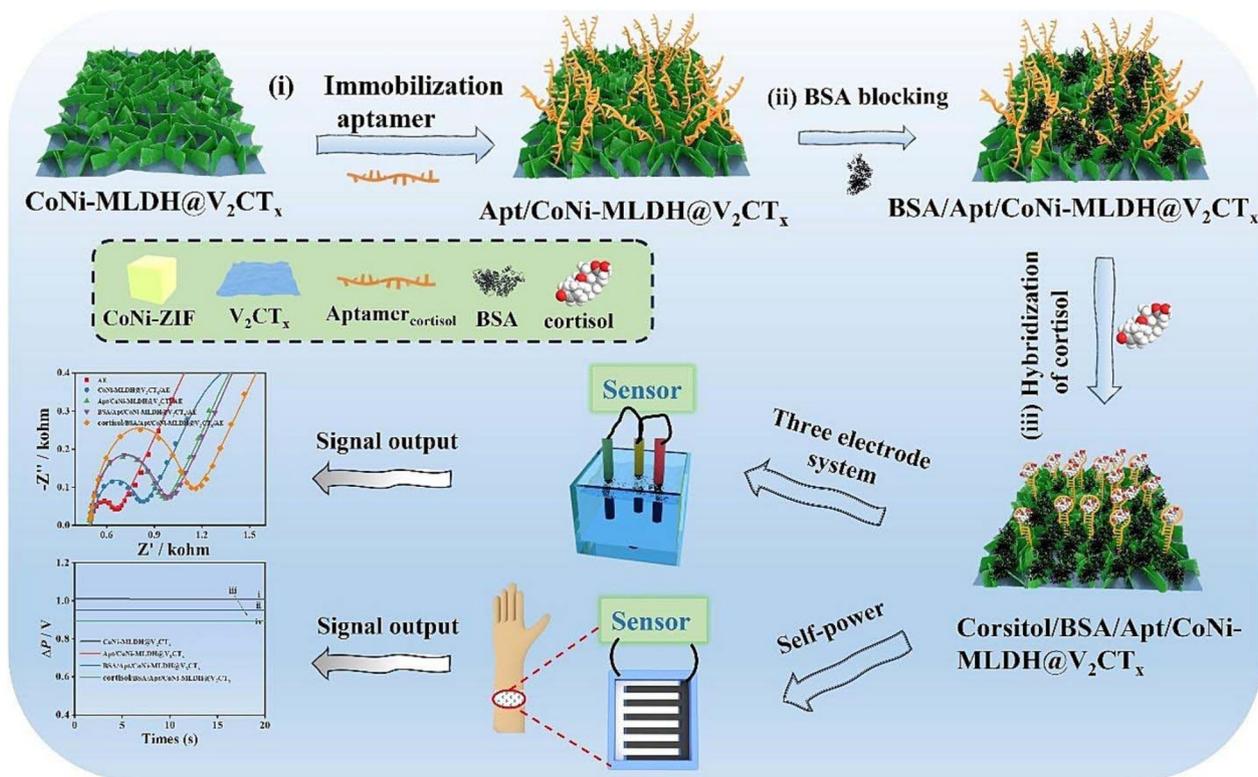

Fig. 4 Schematic illustrations of the design and preparation of the CoNi-MLDH@V$_2$CT$_x$-based aptasensor, with the mechanism of the noninvasive point-of-care cortisol detection. Reprinted (reproduced) with permission from ref. 77, Copyright 2024, Elsevier.

sites, and improved electron transfer reactions, contributing to the aptasensor's high sensitivity and electrocatalytic activity. After optimizing the fabrication and analysis parameters, the aptasensor demonstrated a broad linear detection range from 1.0 pM to 1.0 μM and achieved an ultra-low detection limit of 18 pM. The sensor also showcased excellent accuracy, specificity, and stability during response measurements. Its effectiveness in detecting TOB in human serum samples highlights its potential for clinical applications in monitoring various antibiotics.

To address the critical demand for efficient, simultaneous detection of multiple mycotoxins, commonly found together in food and feed products, a novel MXene-based electrochemical aptasensor array (MBEAA) was developed.[79] This innovative aptasensor array employs highly specific aptamers as recognition elements to detect electrical signal variations in response to target mycotoxins. Utilizing this platform, a multichannel, portable electrochemical device was created, capable of rapidly and cost-effectively detecting aflatoxin B1 (AFB1), ochratoxin A (OTA), and zearalenone (ZEN) simultaneously. The system demonstrated an impressive detection range of 1.0 × 10⁻¹ to 10.0 ng mL⁻¹, with exceptional sensitivity, achieving ultra-low detection limits of 41.2 pg mL⁻¹ for AFB1, 27.6 pg mL⁻¹ for OTA, and 33.0 pg mL⁻¹ for ZEN. Its application in corn sample analysis confirmed the method's effectiveness as a portable, user-friendly, and economical tool for multi-mycotoxin detection. Additionally, this self-developed detection system holds the potential to expand its functionality for detecting a variety of different targets, contingent upon the availability of specific aptamers or antibodies.

A highly sensitive electrochemical aptasensor for the detection of mucin 1 (MUC1) was developed, utilizing MXene/MoS$_2$/PdPtNPs nanomaterials in combination with a hybridization chain reaction (HCR).[80] The MXene/MoS$_2$/PdPtNPs nanocomposite was synthesized through a simple hydrothermal and reduction process, serving as the foundation for the biosensor. The integration of MXene with MoS$_2$-PdPtNPs prevented MXene from curling and simultaneously increased the number of active sites, significantly enhancing electrochemical performance. Upon MUC1 binding to the aptamer, a dsDNA structural switch occurred, leading to the release of aptamers from the electrode surface and triggering the assembly of initiator S, hairpin probe 1 (H1), and hairpin probe 2 (H2) on the electrode, initiating the HCR. The interaction of manganese(III) *meso*-tetrakis (4-N-methylpyridyl)-porphyrin (MnTMPyP) with DNA nanoladders, combined with the PdPtNPs, resulted in a substantial current response in the hydrogen peroxide hydroquinone system. For MUC1 detection, this biosensor demonstrated an impressive linear range of 1 pg mL⁻¹ to 10 ng mL⁻¹, along with a remarkably low detection limit of 0.36 pg mL⁻¹ (S/N = 3). This sensor shows promise for applications in biotechnology and clinical diagnostics.

Amoxicillin, a widely used antibiotic from the penicillin class, is commonly prescribed for treating bacterial infections in areas such as the ear, nose, throat, urinary tract, and skin.[81,82] Due to its extensive use in healthcare, agriculture, environmental, and food-related fields, accurate and sensitive methods for detecting amoxicillin residues are essential. A study presents an innovative fluorescent aptasensor, utilizing FRET, designed specifically for the selective detection of amoxicillin.[83] The sensor operates with a carboxyfluorescein-labeled aptamer as the energy donor and MXene as the energy acceptor and fluorescence quencher. A dual optimization approach, involving response surface methodology with central composite design (RSM-CCD) and artificial neural network-genetic algorithm (ANN-GA), was employed to refine the experimental parameters for maximum detection performance. Fluorescence analysis demonstrated a wide linear detection range from 100 to 2400 ng mL⁻¹ and an impressively low detection limit of 1.53 ng mL⁻¹. The aptasensor showed high selectivity for amoxicillin over other antibiotics typically present in water samples and demonstrated stability and reproducibility. Testing in real water samples confirmed the sensor's reliability, highlighting its potential for precise amoxicillin monitoring in wastewater.

Detecting trace residues of paraquat (PQ) in complex matrices remains crucial for food safety and environmental monitoring.[84–86] To address this need, a novel electrochemical aptasensor was developed using a 3D nanocake-like Au–MXene and Au pallet (Au–MXene/AuP) nanocomposite modified on a SPCE.[87] This aptasensor, constructed through a self-assembly process, leverages the exceptional electrochemical properties of the Au–MXene nanocomposites and AuP substrate-such as high conductivity and extensive surface area—to enable ultrasensitive, label-free detection of PQ. The Apt/Au-MXene/AuP/SPCE-based aptasensor demonstrated strong specificity, anti-interference capacity, repeatability, and stability. A linear correlation was observed between the log-transformed current intensity change [lg(ΔI)] and the log-transformed PQ concentration [lg(CPQ)] across a detection range of 0.05–1000 ng mL⁻¹. The sensor achieved a remarkably low detection limit of 0.028 ng mL⁻¹ and a sensitivity of 255.5 μA (μM cm²)⁻¹. Validated in malt and mint samples, this aptasensor proved highly accurate in complex food matrices, showcasing its potential as a universal analytical platform for detecting trace pesticide residues in diverse food samples by simply swapping the corresponding aptamers.

T-2 toxin is a widely distributed mycotoxin that poses a significant threat to human health through its contamination of field crops and stored grains.[88] In response to this concern, a novel study presents an innovative ECL aptasensor specifically designed for the sensitive detection of T-2 toxin.[89] This aptasensor harnesses the exceptional properties of Ti$_3$C$_2$ MXene nanomaterials, which are functionalized with gold nanorods (AuNRs) and the luminescent indicator Ru(bpy)$_3$²⁺, resulting in a novel Ti$_3$C$_2$@AuNRs-Ru composite. The process begins with the *in situ* growth of gold nanorods on the surface of Ti$_3$C$_2$ MXene, which enhances the surface area and electrochemical properties of the sensor. Ru(bpy)$_3$²⁺ is then electrostatically attached to the Ti$_3$C$_2$@AuNRs, creating a robust luminescent probe that is subsequently immobilized on the electrode surface. This composite structure benefits from the

excellent conductivity and high catalytic activity of MXene, significantly boosting the sensor's sensitivity. To ensure specific binding, the T-2 toxin aptamer is covalently linked to the electrode through Au–S bonds, establishing a solid foundation for the detection mechanism. Following this, a complementary capture DNA (cDNA) strand is introduced, which is paired with a ferrocene-based quenching probe. Ferrocene plays a critical role by quenching the luminescence of the Ti_3C_2@AuNRs-Ru probe, thereby diminishing the ECL signal. When T-2 toxin is present, it competes with the quenching probe for binding to the aptamer. Due to the higher affinity of T-2 toxin for the aptamer, it effectively displaces the quenching probe, leading to a recovery of the ECL signal. This interaction results in a linear correlation between the intensity of the ECL signal and the logarithm of the T-2 toxin concentration, with a detection range spanning from 50 fg mL^{-1} to 50 ng mL^{-1} and an impressive detection limit of 6.44 fg mL^{-1}. The design and implementation of this ECL aptasensor exemplify the integration of advanced nanomaterials and biochemical recognition strategies, providing a highly sensitive method for detecting hazardous pollutants in various matrices. Its successful application to real sample analysis underscores the potential of this innovative approach as a powerful tool for ensuring food safety and protecting public health against the risks posed by mycotoxin contamination.

5.   Conclusion and future perspective

The exploration of MXenes has opened exciting avenues for enhancing diagnostic technologies, particularly through their integration into biosensors. The remarkable versatility of MXenes, combined with their ability to be engineered for specific applications, positions them as powerful tools in the development of advanced diagnostic platforms. Their unique properties, including customizable surface functionalization and variable electrical conductivity, make them ideal candidates for sensitive and selective detection of a wide range of analytes. Looking ahead, future research should focus on several key areas to fully realize the potential of MXenes in biosensing applications. First, there is a need for further development of scalable synthesis methods that ensure consistency and reproducibility of MXene materials for commercial use. Additionally, exploring novel surface modifications and functionalization strategies could enhance the specificity and sensitivity of biosensors, enabling the detection of even more complex and low-abundance analytes. The integration of MXenes with emerging technologies such as wearable sensors, aptamer science, and point-of-care devices could also revolutionize real-time health monitoring and personalized medicine. Furthermore, interdisciplinary collaboration between materials scientists, chemists, and biomedical engineers will be crucial in addressing the challenges associated with the deployment of MXenes in practical applications. Continued research into the long-term stability and biocompatibility of MXene-based aptasensors will ensure their safe and effective use in diverse environments. MXenes hold significant promise for advancing diagnostic technologies and improving public health. By addressing current challenges and leveraging their unique properties, the future of MXene-based aptasensors looks exceptionally bright, with the potential to transform the early detection and monitoring of diseases on a global scale.

Data availability

There is no data associated with this review manuscript.

Conflicts of interest

There are no conflicts to declare.

References

1 H. Altug, S.-H. Oh, S. A. Maier and J. Homola, Advances and applications of nanophotonic biosensors, *Nat. Nanotechnol.*, 2022, **17**(1), 5–16.

2 A. Williams, M. R. Aguilar, K. G. Pattiya Arachchillage, S. Chandra, S. Rangan, S. Ghosal Gupta and J. M. Artes Vivancos, Biosensors for Public Health and Environmental Monitoring: The Case for Sustainable Biosensing, *ACS Sustainable Chem. Eng.*, 2024, **12**(28), 10296–10312.

3 M. R. Ali, M. S. Bacchu, M. R. Al-Mamun, M. I. Hossain, A. Khaleque, A. Khatun, D. D. Ridoy, M. A. S. Aly and M. Z. H. Khan, Recent advanced in MXene research toward biosensor development, *Crit. Rev. Anal. Chem.*, 2022, 1–18.

4 U. Amara, I. Hussain, M. Ahmad, K. Mahmood and K. Zhang, 2D MXene–based biosensing: a review, *Small*, 2023, **19**(2), 2205249.

5 B. Xu, C. Zhi and P. Shi, Latest advances in MXene biosensors, *J. Phys.: Mater.*, 2020, **3**(3), 031001.

6 M. Mathew and C. S. Rout, Electrochemical biosensors based on Ti3C2Tx MXene: future perspectives for on-site analysis, *Curr. Opin. Electrochem.*, 2021, **30**, 100782.

7 H. L. Chia, C. C. Mayorga-Martinez, N. Antonatos, Z. k. Sofer, J. J. Gonzalez-Julian, R. D. Webster and M. Pumera, MXene titanium carbide-based biosensor: strong dependence of exfoliation method on performance, *Anal. Chem.*, 2020, **92**(3), 2452–2459.

8 A. Parihar, A. Singhal, N. Kumar, R. Khan, M. A. Khan and A. K. Srivastava, Next-generation intelligent MXene-based electrochemical aptasensors for point-of-care cancer diagnostics, *Nano-Micro Lett.*, 2022, **14**(1), 100.

9 A. Parihar, N. K. Choudhary, P. Sharma and R. Khan, MXene-based aptasensor for the detection of aflatoxin in food and agricultural products, *Environ. Pollut.*, 2023, **316**, 120695.

10 A. Parihar, P. Vishwakarma and R. Khan, MXenes-based hybrid electrochemical sensors for cancer diagnostics, in *Mxene-Based Hybrid Nano-Architectures for Environmental*

Remediation and Sensor Applications, Elsevier, 2024, pp. 287–304.

11 L. Pauling and R. B. Corey, A proposed structure for the nucleic acids, *Proc. Natl. Acad. Sci. U. S. A.*, 1953, **39**(2), 84–97.

12 R. Micura and C. Höbartner, Fundamental studies of functional nucleic acids: aptamers, riboswitches, ribozymes and DNAzymes, *Chem. Soc. Rev.*, 2020, **49**(20), 7331–7353.

13 D. P. Horning and G. F. Joyce, Amplification of RNA by an RNA polymerase ribozyme, *Proc. Natl. Acad. Sci. U. S. A.*, 2016, **113**(35), 9786–9791.

14 M. Famulok, J. S. Hartig and G. Mayer, Functional aptamers and aptazymes in biotechnology, diagnostics, and therapy, *Chem. Rev.*, 2007, **107**(9), 3715–3743.

15 S. C. B. Gopinath, Methods developed for SELEX, *Anal. Bioanal. Chem.*, 2007, **387**, 171–182.

16 M. Darmostuk, S. Rimpelova, H. Gbelcova and T. Ruml, Current approaches in SELEX: An update to aptamer selection technology, *Biotechnol. Adv.*, 2015, **33**(6), 1141–1161.

17 M. Famulok and G. Mayer, Aptamers and SELEX in chemistry & biology, *Chem. Biol.*, 2014, **21**(9), 1055–1058.

18 X. Li, J. Wang, G. Yang, X. Fang, L. Zhao, Z. Luo and Y. Dong, The Development of Aptamer-Based Gold Nanoparticle Lateral Flow Test Strips for the Detection of SARS-CoV-2 S Proteins on the Surface of Cold-Chain Food Packaging, *Molecules*, 2024, **29**(8), 1776.

19 V. Crivianu-Gaita and M. Thompson, Aptamers, antibody scFv, and antibody Fab'fragments: An overview and comparison of three of the most versatile biosensor biorecognition elements, *Biosens. Bioelectron.*, 2016, **85**, 32–45.

20 S. Y. Toh, M. Citartan, S. C. Gopinath and T.-H. Tang, Aptamers as a replacement for antibodies in enzyme-linked immunosorbent assay, *Biosens. Bioelectron.*, 2015, **64**, 392–403.

21 Z. Huang, L. Qiu, T. Zhang and W. Tan, Integrating DNA nanotechnology with aptamers for biological and biomedical applications, *Matter*, 2021, **4**(2), 461–489.

22 N. Rabiee, S. Ahmadi, Z. Arab, M. Bagherzadeh, M. Safarkhani, B. Nasseri, M. Rabiee, M. Tahriri, T. J. Webster and L. Tayebi, Aptamer hybrid nanocomplexes as targeting components for antibiotic/gene delivery systems and diagnostics: a review, *Int. J. Nanomed.*, 2020, 4237–4256.

23 N. Rabiee, S. Chen, S. Ahmadi and R. N. Veedu, Aptamer-engineered (nano) materials for theranostic applications, *Theranostics*, 2023, **13**(15), 5183.

24 M. Safarkhani, S. Ahmadi, H. Ipakchi, M. R. Saeb, P. Makvandi, M. Ebrahimi Warkiani, N. Rabiee and Y. Huh, Advancements in Aptamer–Driven DNA Nanostructures for Precision Drug Delivery, *Adv. Sci.*, 2024, 2401617.

25 S. Maghsoudi, B. T. Shahraki, N. Rabiee, R. Afshari, Y. Fatahi, R. Dinarvand, S. Ahmadi, M. Bagherzadeh, M. Rabiee and L. Tayebi, Recent advancements in aptamer-bioconjugates: sharpening stones for breast and prostate cancers targeting, *J. Drug Delivery Sci. Technol.*, 2019, **53**, 101146.

26 P. Röthlisberger and M. Hollenstein, Aptamer chemistry, *Adv. Drug Delivery Rev.*, 2018, **134**, 3–21.

27 J. P. Elskens, J. M. Elskens and A. Madder, Chemical modification of aptamers for increased binding affinity in diagnostic applications: Current status and future prospects, *Int. J. Mol. Sci.*, 2020, **21**(12), 4522.

28 H. Yu, J. Zhu, G. Shen, Y. Deng, X. Geng and L. Wang, Improving aptamer performance: key factors and strategies, *Microchim. Acta*, 2023, **190**(7), 255.

29 V. Esposito, M. Scuotto, A. Capuozzo, R. Santamaria, M. Varra, L. Mayol, A. Virgilio and A. Galeone, A straightforward modification in the thrombin binding aptamer improving the stability, affinity to thrombin and nuclease resistance, *Org. Biomol. Chem.*, 2014, **12**(44), 8840–8843.

30 R. Dolot, C. H. Lam, M. Sierant, Q. Zhao, F.-W. Liu, B. Nawrot, M. Egli and X. Yang, Crystal structures of thrombin in complex with chemically modified thrombin DNA aptamers reveal the origins of enhanced affinity, *Nucleic Acids Res.*, 2018, **46**(9), 4819–4830.

31 S. O. Lee and S. D. Fried, An error prone PCR method for small amplicons, *Anal. Biochem.*, 2021, **628**, 114266.

32 M. Mousivand, L. Anfossi, K. Bagherzadeh, N. Barbero, A. Mirzadi-Gohari and M. Javan-Nikkhah, In silico maturation of affinity and selectivity of DNA aptamers against aflatoxin B1 for biosensor development, *Anal. Chim. Acta*, 2020, **1105**, 178–186.

33 A. He, L. Wan, Y. Zhang, Z. Yan, P. Guo, D. Han and W. Tan, Structure-based investigation of a DNA aptamer targeting PTK7 reveals an intricate 3D fold guiding functional optimization, *Proc. Natl. Acad. Sci. U. S. A.*, 2024, **121**(29), e2404060121.

34 T. L. Bullock, L. D. Sherlin and J. J. Perona, Tertiary core rearrangements in a tight binding transfer RNA aptamer, *Nat. Struct. Biol.*, 2000, **7**(6), 497–504.

35 M. Vorobyeva, P. Vorobjev and A. Venyaminova, Multivalent aptamers: Versatile tools for diagnostic and therapeutic applications, *Molecules*, 2016, **21**(12), 1613.

36 T. Wang, M. P. Gantier, D. Xiang, A. G. Bean, M. Bruce, S.-F. Zhou, M. Khasraw, A. Ward, L. Wang and M. Q. Wei, EpCAM aptamer-mediated survivin silencing sensitized cancer stem cells to doxorubicin in a breast cancer model, *Theranostics*, 2015, **5**(12), 1456.

37 S. Ni, H. Yao, L. Wang, J. Lu, F. Jiang, A. Lu and G. Zhang, Chemical modifications of nucleic acid aptamers for therapeutic purposes, *Int. J. Mol. Sci.*, 2017, **18**(8), 1683.

38 H. Jo and C. Ban, Aptamer–nanoparticle complexes as powerful diagnostic and therapeutic tools, *Exp. Mol. Med.*, 2016, **48**(5), e230–e230.

39 D. W. Drolet, J. Nelson, C. E. Tucker, P. M. Zack, K. Nixon, R. Bolin, M. B. Judkins, J. A. Farmer, J. L. Wolf and S. C. Gill, Pharmacokinetics and safety of an anti-vascular endothelial growth factor aptamer (NX1838) following injection into the vitreous humor of rhesus monkeys, *Pharm. Res.*, 2000, **17**, 1503–1510.

40 P. R. Mallikaratchy, A. Ruggiero, J. R. Gardner, V. Kuryavyi, W. F. Maguire, M. L. Heaney, M. R. McDevitt, D. J. Patel

and D. A. Scheinberg, A multivalent DNA aptamer specific for the B-cell receptor on human lymphoma and leukemia, *Nucleic Acids Res.*, 2011, **39**(6), 2458–2469.

41 M. Naguib, M. Kurtoglu, V. Presser, J. Lu, J. Niu, M. Heon, L. Hultman, Y. Gogotsi and M. W. Barsoum, Two–dimensional nanocrystals: two-dimensional nanocrystals produced by exfoliation of Ti3AlC2 (Adv. Mater. 37/2011), *Adv. Mater.*, 2011, **23**(37), 4207–4207.

42 M. Naguib, O. Mashtalir, J. Carle, V. Presser, J. Lu, L. Hultman, Y. Gogotsi and M. W. Barsoum, Two-dimensional transition metal carbides, *ACS Nano*, 2012, **6**(2), 1322–1331.

43 G. Deysher, C. E. Shuck, K. Hantanasirisakul, N. C. Frey, A. C. Foucher, K. Maleski, A. Sarycheva, V. B. Shenoy, E. A. Stach and B. Anasori, Synthesis of Mo4VAlC4 MAX phase and two-dimensional Mo4VC4 MXene with five atomic layers of transition metals, *ACS Nano*, 2019, **14**(1), 204–217.

44 B. Anasori, Y. Xie, M. Beidaghi, J. Lu, B. C. Hosler, L. Hultman, P. R. Kent, Y. Gogotsi and M. W. Barsoum, Two-dimensional, ordered, double transition metals carbides (MXenes), *ACS Nano*, 2015, **9**(10), 9507–9516.

45 A. VahidMohammadi, J. Rosen and Y. Gogotsi, The world of two-dimensional carbides and nitrides (MXenes), *Science*, 2021, **372**(6547), eabf1581.

46 A. T. Wee, M. C. Hersam, M. Chhowalla and Y. Gogotsi, *An update from Flatland*, ACS Publications, 2016, vol. 10, pp. 8121–8123.

47 H. Zhang, Ultrathin two-dimensional nanomaterials, *ACS Nano*, 2015, **9**(10), 9451–9469.

48 K. J. Koski and Y. Cui, The new skinny in two-dimensional nanomaterials, *ACS Nano*, 2013, **7**(5), 3739–3743.

49 M. Ghidiu, M. R. Lukatskaya, M.-Q. Zhao, Y. Gogotsi and M. W. Barsoum, Conductive two-dimensional titanium carbide 'clay'with high volumetric capacitance, in *MXenes*, Jenny Stanford Publishing, 2023, pp. 379–399.

50 B. Lalmi, H. Oughaddou, H. Enriquez, A. Kara, S. Vizzini, B. Ealet and B. Aufray, Epitaxial growth of a silicene sheet, *Appl. Phys. Lett.*, 2010, **97**(22), 223109.

51 X. Li, Z. Huang, C. E. Shuck, G. Liang, Y. Gogotsi and C. Zhi, MXene chemistry, electrochemistry and energy storage applications, *Nat. Rev. Chem.*, 2022, **6**(6), 389–404.

52 K. R. G. Lim, M. Shekhirev, B. C. Wyatt, B. Anasori, Y. Gogotsi and Z. W. Seh, Fundamentals of MXene synthesis, *Nat. Synth.*, 2022, **1**(8), 601–614.

53 K. Khan, A. K. Tareen, M. Iqbal, I. Hussain, A. Mahmood, U. Khan, M. F. Khan, H. Zhang and Z. Xie, Recent advances in MXenes: a future of nanotechnologies, *J. Mater. Chem. A*, 2023, **11**, 19764–19811.

54 J. Cao, T. Li, H. Gao, Y. Lin, X. Wang, H. Wang, T. Palacios and X. Ling, Realization of 2D crystalline metal nitrides via selective atomic substitution, *Sci. Adv.*, 2020, **6**(2), eaax8784.

55 A. M. Patil, A. A. Jadhav, N. R. Chodankar, A. T. Avatare, J. Hong, S. D. Dhas, U. M. Patil and S. C. Jun, Recent progress of MXene synthesis, properties, microelectrode fabri-

cation techniques for microsupercapacitors and microbatteries energy storage devices and integration: A comprehensive review, *Coord. Chem. Rev.*, 2024, **517**, 216020.

56 Y. Chen, H. Qin, J. Zhou, T. Yang, B. Sun, Y. Ni, H. Wang, S. A. Redfern, M. Miao and H.-Q. Lin, Unveiling interstitial anionic electron-driven ultrahigh K-ion storage capacity in a novel two-dimensional electride exemplified by Sc3Si2, *J. Phys. Chem. Lett.*, 2022, **13**(32), 7439–7447.

57 M. Khazaei, J. Wang, M. Estili, A. Ranjbar, S. Suehara, M. Arai, K. Esfarjani and S. Yunoki, Novel MAB phases and insights into their exfoliation into 2D MBenes, *Nanoscale*, 2019, **11**(23), 11305–11314.

58 Y. Yin, Q. Gong, M. Yi and W. Guo, Emerging versatile two-dimensional MoSi2N4 family, *Adv. Funct. Mater.*, 2023, **33**(26), 2214050.

59 T. Latychevskaia, D. Bandurin and K. Novoselov, A new family of septuple-layer 2D materials of MoSi2N4-like crystals, *Nat. Rev. Phys.*, 2024, 1–13.

60 A. Sharma, V. Rangra and A. Thakur, Synthesis, properties, and applications of MBenes (two-dimensional metal borides) as emerging 2D materials: a review, *J. Mater. Sci.*, 2022, **57**(27), 12738–12751.

61 T. Xu, Y. Wang, Z. Xiong, Y. Wang, Y. Zhou and X. Li, A rising 2D star: novel MBenes with excellent performance in energy conversion and storage, *Nano-Micro Lett.*, 2023, **15**(1), 6.

62 A. Zarepour, S. Ahmadi, N. Rabiee, A. Zarrabi and S. Iravani, Self-healing MXene-and graphene-based composites: properties and applications, *Nano-Micro Lett.*, 2023, **15**(1), 100.

63 M. Safarkhani, B. F. Far, Y. Huh and N. Rabiee, Thermally conductive MXene, *ACS Biomater. Sci. Eng.*, 2023, **9**(12), 6516–6530.

64 M. R. Farani, B. N. Khiarak, R. Tao, Z. Wang, S. Ahmadi, M. Hassanpour, M. Rabiee, M. R. Saeb, E. C. Lima and N. Rabiee, 2D MXene nanocomposites: electrochemical and biomedical applications, *Environ. Sci.: Nano*, 2022, **9**(11), 4038–4068.

65 Y. Li, J. Li, L. Wan, J. Li, H. Qu, C. Ding, M. Li, D. Yu, K. Fan and H. Yao, The first-principle study on tuning optical properties of MA2Z4 by Cr replacement of Mo atoms in MoSi2N4, *Nanomaterials*, 2022, **12**(16), 2822.

66 X. Sun, J. Zheng, Z. Yao, S. Deng, Z. Pan, S. Wang and J. Wang, DFT investigation of single metal atom-doped 2D MA2Z4 materials for NO electrocatalytic reduction to NH3, *J. Phys. Chem. C*, 2022, **126**(41), 17598–17607.

67 N. Kwon, S. Lee, M. Jang, J.-H. Lee, C. Park and T. Lee, Synthesis of truncated DNA aptamer and its application to an electrochemical biosensor consisting of an aptamer and a MXene heterolayer for yellow fever virus, *BioChip J.*, 2024, **18**(1), 93–102.

68 H. Duan, S.-Y. Tang, K. Goda and M. Li, Enhancing the sensitivity and stability of electrochemical aptamer-based sensors by AuNPs@ MXene nanocomposite for continuous monitoring of biomarkers, *Biosens. Bioelectron.*, 2024, **246**, 115918.

69 H. Zhang, M. Zhang, Z. Yu, Y. Zhou, Y. Hu, L. Gao, L. Cao, H. Yin and S. Ai, MXene-enhanced Bi2S3/CdIn2S4 heterojunction photosensitive gate for DEHP detection in a signal-on OPECT aptamer biosensor, *Anal. Chem.*, 2024, **96**(5), 1948–1956.

70 S. Xiong, Z. Wu, F. Li, P. Zhao, H. Li, H. Bao and X. Yang, Self-assembled sensing interface based on specific aptamer functionalized Ti3C2 MXene for ultrasensitive antibiotic detection in milk, *LWT–Food Sci. Technol.*, 2024, **200**, 116186.

71 K. Zhao, B. Zhang, X. Cui, X. Chao, F. Song, H. Chen and B. He, An electrochemical aptamer-sensing strategy based on a Ti3C2Tx MXene synergistic Ti-MOF amplification signal for highly sensitive detection of zearalenone, *Food Chem.*, 2024, 140828.

72 Z. Wang, S. Liu, Z. Shi, D. Lu, Z. Li and Z. Zhu, Electrochemical biosensor based on RNA aptamer and ferrocenecarboxylic acid signal probe for C-reactive protein detection, *Talanta*, 2024, 126318.

73 M. Ghalkhani, F. Mollaie, F. Nosratzehi, E. Sohouli and F. Ahmadi, Preparation of Mxene-AuNPs/TGA nanocomposites explored as an electrochemical aptasensor for Digoxin analysis, *Microchem. J.*, 2024, **205**, 111196.

74 H. Cui, T. Zheng, N. Qian, X. Fu, A. Li, S. Xing and X. F. Wang, Aptamer–Functionalized Magnetic Ti3C2 Based Nanoplatform for Simultaneous Enrichment and Detection of Exosomes, *Small*, 2024, 2402434.

75 C. Ye, M. Wang, J. Min, R. Y. Tay, H. Lukas, J. R. Sempionatto, J. Li, C. Xu and W. Gao, A wearable aptamer nanobiosensor for non-invasive female hormone monitoring, *Nat. Nanotechnol.*, 2024, **19**(3), 330–337.

76 T. Jinsong, H. Jin, L. Weizhang, C. Junyou, L. Jian, C. Xiangming and Z. Hua, Integrating MXene/MWCNTs into aptasensor capable of ultrasensitive quantification of cTnI towards the diagnosis of acute myocardial infarction, *Chem. Pap.*, 2024, **78**(5), 3205–3212.

77 J. Liu, Z. Tao, Y. Zhang, T. Ni, B. Liu and Z. Zhang, Dual-modal flexible zinc-air battery-driven self-powered and impedimetric aptasensor based on the hybrid of V2CTx MXene and bimetallic layered double hydroxide for the detection of cortisol, *Microchem. J.*, 2024, **197**, 109757.

78 F. Nasri, M. Hosseini, S. M. Taghdisi, M. R. Ganjali and M. Ramezani, Design and application of an ultrasensitive and selective tobromycin electrochemiluminescence aptasensor using MXene/Ni/Sm-LDH-based nanocomposite, *Microchim. Acta*, 2024, **191**(9), 506.

79 C. Wang, X. Zhao, X. Huang, F. Xu, C. Gu, S. Yu, X. Zhang and J. Qian, Simultaneous detection of multiple mycotoxins using MXene-based electrochemical aptasensor array and a self-developed multi-channel portable device, *Talanta*, 2024, **278**, 126450.

80 X. Xu, N. Li, J. Huang, T. Zhu, X. Su, Y. Ma, R. Yang, J. Ruan and H. Su, The novel few layered MXene/MoS2/PdPtNPs nanomaterials combined with hybrid chain reaction for electrochemical detection of mucin 1, *Microchem. J.*, 2024, **197**, 109827.

81 A. M. Geddes, K. P. Klugman and G. N. Rolinson, Introduction: historical perspective and development of amoxicillin/clavulanate, *Int. J. Antimicrob. Agents*, 2007, **30**, 109–112.

82 F. Salvo, A. De Sarro, A. P. Caputi and G. Polimeni, Amoxicillin and amoxicillin plus clavulanate: a safety review, *Expert Opin. Drug Saf.*, 2009, **8**(1), 111–118.

83 M. Zermane, M. Berkani, A. Teniou, T. M. Aminabhavi, Y. Vasseghian, G. Catanante, N. Lakhdari and A. Rhouati, Modeling approach for Ti3C2 MXene-based fluorescent aptasensor for amoxicillin biosensing in water matrices, *J. Environ. Manage.*, 2024, **360**, 121072.

84 C. Berry, C. La Vecchia and P. Nicotera, Paraquat and Parkinson's disease, *Cell Death Differ.*, 2010, **17**(7), 1115–1125.

85 R. Dinis-Oliveira, F. Remiao, H. Carmo, J. Duarte, A. S. Navarro, M. Bastos and F. Carvalho, Paraquat exposure as an etiological factor of Parkinson's disease, *Neurotoxicology*, 2006, **27**(6), 1110–1122.

86 R. Dinis-Oliveira, J. Duarte, A. Sánchez-Navarro, F. Remião, M. Bastos and F. Carvalho, Paraquat poisonings: mechanisms of lung toxicity, clinical features, and treatment, *Crit. Rev. Toxicol.*, 2008, **38**(1), 13–71.

87 Q.-B. Xu, J. Wang, P.-Y. Song, Y. Li, N. Long, W.-J. Wu, L.-D. Zhou, L.-C. Shi, R.-L. Pan and W.-J. Kong, 3D nano-cake-like Au-MXene/Au pallet structure–based label-free electrochemical aptasensor for paraquat determination, *Microchim. Acta*, 2024, **191**(1), 33.

88 Y. Li, Z. Wang, R. C. Beier, J. Shen, D. D. Smet, S. De Saeger and S. Zhang, T-2 toxin, a trichothecene mycotoxin: review of toxicity, metabolism, and analytical methods, *J. Agric. Food Chem.*, 2011, **59**(8), 3441–3453.

89 J. Zhang, Y. Deng, L. Chen, F. Luo, Z. Weng, C. Lin, B. Qiu, L. Guo and Z. Lin, A novel electrochemiluminescence aptasensor using Ti3C2@ AuNRs-Ru for ultra-sensitive detection of T-2 toxin, *Electrochim. Acta*, 2024, **475**, 143688.